JOURNAL OF SOLID STATE CHEMISTRY 65, 293–300 (1986)

Sodium Motion in the Nasicon Related $Na_{1+x}Zr_{2-x}In_x(PO_4)_3$ Solid Solution: An NMR Study

F. CHERKAOUI, G. VILLENEUVE, C. DELMAS,
AND P. HAGENMULLER

Laboratoire de Chimie du Solide du CNRS, Université de Bordeaux I 351, cours de la Libération 33405 Talence Cedex, France

Received December 24, 1985

Sodium ion motion in $Na_{1+x}Zr_{2-x}In_x(PO_4)_3$ Nasicon-related materials ($0 \le x \le 1.85$) has been studied by NMR at two resonance frequencies from 170 to 450 K. At 8 MHz the resonance lines due to $M1$- and $M2$-type sites are well resolved. They are split by a strong second-order quadrupolar effect ($\nu_Q = 1.5$ Megacycles (Mc)/sec). For $NaZr_2(PO_4)_3$ only the $M1$ site is occupied at *RT*, while a new site $M5$ appears at rising temperature (410 K). At 21 Mc/sec the line narrowing observed at increasing temperature illustrates the Na^+ ion mobility within the skeleton. According to the temperature and the value of the ionic conductivity two diffusion mechanisms seem to occur. © 1986 Academic Press, Inc.

Introduction

Since the discovery by Goodenough, Hong, and Kafalas of the high Na^+ conductivity in the Nasicon type structure, many studies have been devoted to this family of materials (*1, 2*). Most of them concern the highest conductive $Na_3Zr_2Si_2PO_{12}$ phase which belongs in fact to the $Na_{1+x}Zr_2Si_xP_{3-x}O_{12}$ ($0 \le x \le 3$) solid solution.

Due to the lack of single crystals and the complexity of the structure, the exact diffusion mechanism is not well understood and various hypotheses have been proposed (*3–5*). Moreover these difficulties are increased by the occurrence of a Na^+ order–disorder transition when the sodium rate is close to three (*6, 7*).

To get better knowledge of this class of materials, numerous studies have been devoted to other ionic conductors exhibiting this structural type. A few years ago it was shown in this laboratory that the substitution of a trivalent element for Zr^{4+} in $NaZr_2(PO_4)_3$ allows the insertion of sodium ions in the framework (*8, 9*). $Na_3M_2(PO_4)_3$ (M = Ti, V, Cr, Fe) and the $Na_{1+x}Zr_{2-x}L_x(PO_4)_3$ (L = Cr, In, Yb) solid solution have been obtained and characterized from the crystal chemical and ionic conductivity point of view.

Up to now very few NMR studies have been carried out on this type of materials (*10, 11*). Since NMR is sensitive to static and dynamic distribution a general study has been undertaken to determine the relations between diffusion mechanism, conductivity, and composition. Attention has been focused on the simplest materials such as $NaZr_2(PO_4)_3$ and $NaTi_2(PO_4)_3$ and on the $Na_{1+x}Zr_{2-x}In_x(PO_4)_3$ solid solution.

Structure Description

The structure of $NaZr_2(PO_4)_3$, a related material of the same family, has been deter-

0022-4596/86 $3.00
Copyright © 1986 by Academic Press, Inc.
All rights of reproduction in any form reserved.

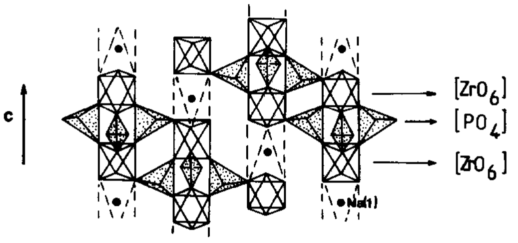

FIG. 1. Polyhedra connected in the $NaZr_2(PO_4)_3$ type structure.

mined by Hagman and Kierkegaard (*12*). It can be described from $O_3ZrO_3Na(M1)$ O_3ZrO_3 groups linked by PO_4^{3-} anions to form infinite ribbons parallel to the *c* axis (Fig. 1). These ribbons are connected by PO_4^{3-} tetrahedra perpendicularly to the *c* direction to build a 3D skeleton (Fig. 2). In the rhombohedral symmetry (space group $R\bar{3}c$) two sites are available in the framework for Na^+ ions. For the $NaZr_2(PO_4)_3$ composition the octahedral $M1(6b)$ site is fully occupied, while the eight fold coordinated $M2(18e)$ position is empty. Figure 3 shows the environment of both sites. Among the 14 oxygens surrounding the $M2$ cavity, only the 8 nearest ($d_{M2\text{-oxyg.}} < 3.0$ Å) (*A-C-J-I-H-G-L-K*) form the coordination polyhedron. This figure has been drawn from the atomic positions published by d'Yvoire *et al.* for γ-$Na_3Cr_2(PO_4)_3$ (*13*). The two possible diffusion jumps, the $M2$–$M2$ direct transfer and the $M1$–$M2$–$M1$ indirect transfer, are represented.

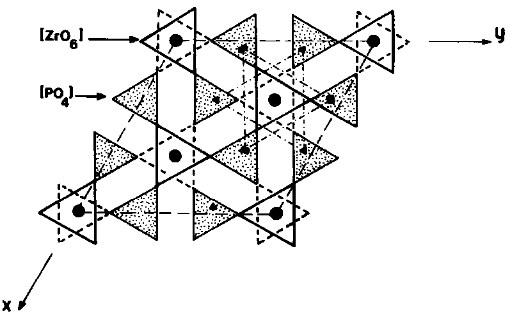

FIG. 2. Projection of the $NaZr_2(PO_4)_3$ type structure on the xOy plane in the vicinity of $z = 0.25$. ● $M1$ site at z; ■ $M2$ site at $z - c_{hex}/12$; ▲ $M2$ site at $z + c_{hex}/12$.

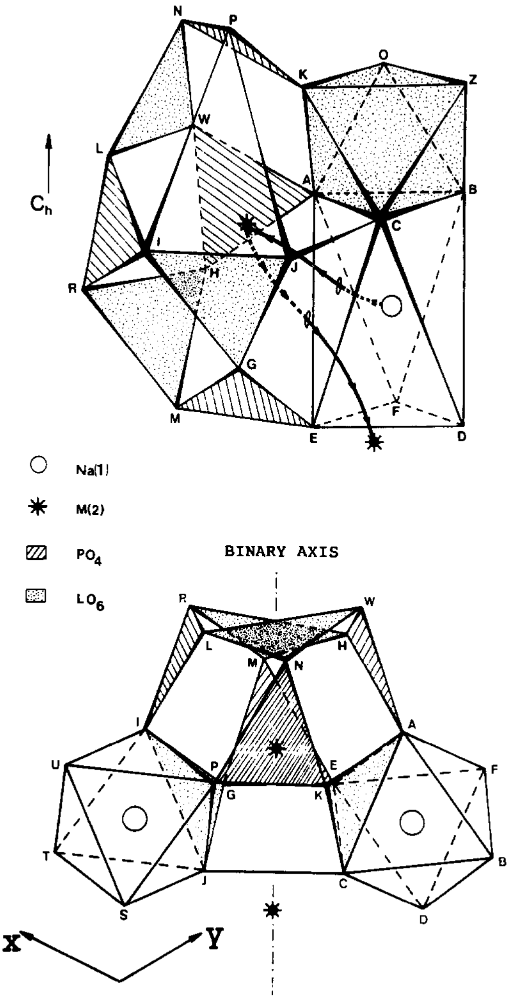

FIG. 3. Surrounding of the $M1$ and $M2$ sites in the Nasicon type structure.

In $NaZr_2(PO_4)_3$ the Na^+–Na^+ interactions are very weak due to the high $M1$–$M1$ distance (11.38 Å).

When the $M2$ site is filling the strong $Na^+(M1)$–$Na^+(M2)$ electrostatic repulsion ($d_{M1\text{–}M2} \simeq 3.38$ Å) brings about a migration of Na^+ ions from $M1$ to $M2$ which decreases the repulsion ($d_{M2\text{–}M2} \simeq 4.71$ Å).

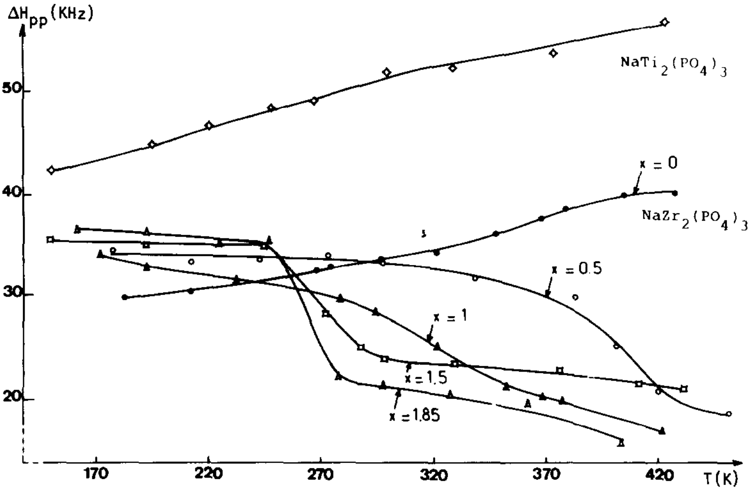

FIG. 4. Variation of the linewidth at 21 Mc/sec vs temperature for $NaTi_2(PO_4)_3$ and for $Na_{1+x}Zr_{2-x}In_x(PO_4)_3$.

Experimental

Materials preparation. All the materials have been elaborated from mixtures of Na_2CO_3, $(NH_4)_2HPO_4$ and TiO_2, ZrO_2, and In_2O_3 oxides in stoichiometric proportions. The mixtures are preheated 10 hr at 200°C to decompose $(NH_4)_2HPO_4$ and 15 hr at 800°C to dissociate Na_2CO_3. Final treatments need 15 hr at 950°C except for $NaTi_2(PO_4)_3$ and $NaZr_2(PO_4)_3$ which need a reaction temperature of 1200°C.

NMR investigation. The ^{23}Na NMR studies were carried out by continuous wave (cw) method, using a cross-coil variable-frequency Bruker SWL 100 spectrometer. The magnetic field was supplied by a Drush magnet and monitored by a Hall probe. Suitable temperatures with fluctuations below 1 K were obtained thanks to a homemade gas flow system blowing the sample.

Experiments were made at 21 and 8 megacycles (Mc)/sec. At the latter frequency, because of the low value of the signal/noise ratio, the spectra were accumulated 64 times, each scan during 10 min. The signal was transferred to a signal averager Nicolet 527, then integrated by a Hewlett-Packard HP 9825 computer.

Results

$NaZr_2(PO_4)_3$

At 21 Mc/sec and at room temperature (295 K) the spectrum is composed of a single broad line ($\Delta H = 3.0$ mT, i.e., 34 kc/sec). This width is too large to be attributed only to dipolar interactions (^{23}Na–^{23}Na and ^{23}Na–^{31}P). One must take into account the second-order quadrupolar broadening corresponding to the unresolved structure of the $\frac{1}{2} \rightarrow \frac{1}{2}$ transition, and the observed width is due to the contribution of both dipolar and quadrupolar effects.

The variation of the linewidth with temperature is given in Fig. 4. One can observe an increase of ΔH from 30 to 40 kc/sec when the temperature increases from 200 to 420 K. This behavior is a priori quite anomalous.

At 8 Mc/sec the second-order quadrupolar structure is well resolved at room temperature (Fig. 5a), with a separation of 140

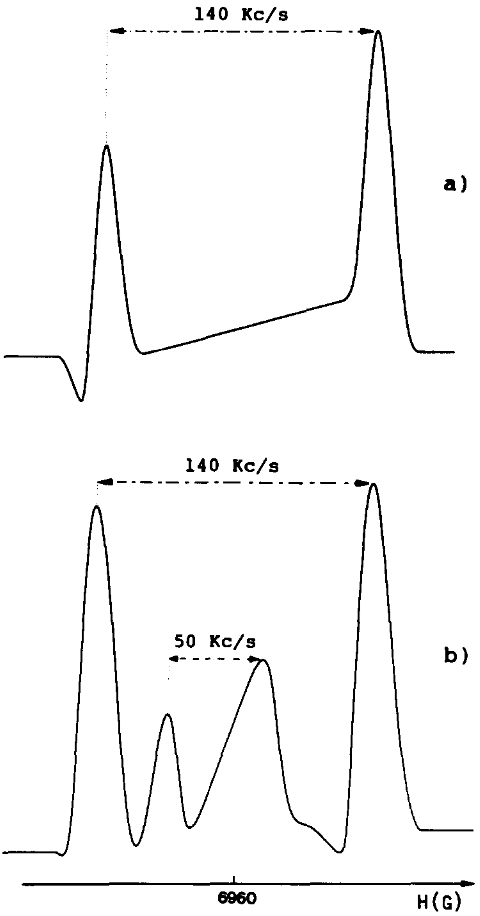

FIG. 5. Shape of the resonance line at 8 Mc/sec for $NaZr_2(PO_4)_3$ (a) at 300 K, (b) at 413 K.

kc/sec between the two maxima. This splitting value can be obviously ascribed to the noncubic symmetry of the $M1$ site occupied by the Na^+ ions. With increasing temperature a second line appears with a splitting of 50 kc/sec (Fig. 5b), which shows the migration of some Na^+ ions from the $M1$ site into a different one.

$Na_{1+x}Zr_{2-x}In_x(PO_4)_3$ *with* $x = 0.5, 1.0, 1.5$ *and* 1.85

At 21 Mc/sec, one can observe the same broad unresolved line as that of $NaZr_2(PO_4)_3$ but a striking difference appears in the thermal behavior. Now the line narrows for each composition when the temperature increases above 250 K, probably due to some motion of Na^+ ions (Figs. 4 and 6). The linewidth decreases to 17 kc/sec at 420 K for the highest sodium concentrations.

At 8 Mc/sec the second-order quadrupolar structure is well resolved even at the lowest investigated temperature (Fig. 7). According to the crystal structure of these phases (*12*, *2*), the line whose splitting is 140 kc/sec is ascribed to Na^+ ions in the $M1$ site, while (as we have seen above) the line whose splitting is 80 kc/sec seems to be due to Na^+ ions in $M2$ sites.

Analysis of the Results

Structural Data

From the spectra obtained at 8 Mc/s, the quadrupolar coupling constant associated with the $M1$ site can be derived. The crystal structure of $NaZr_2(PO_4)_3$ shows that the $M1$ site exhibits an axial symmetry (Fig. 3) so that the asymmetry parameter η vanishes.

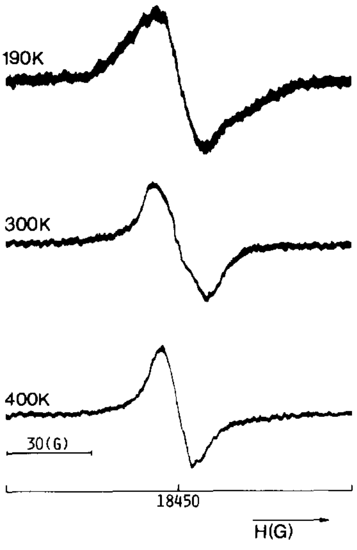

FIG. 6. Thermal modification of the resonance line (derivated) at 21 Mc/sec for $Na_2InZr(PO_4)_3$.

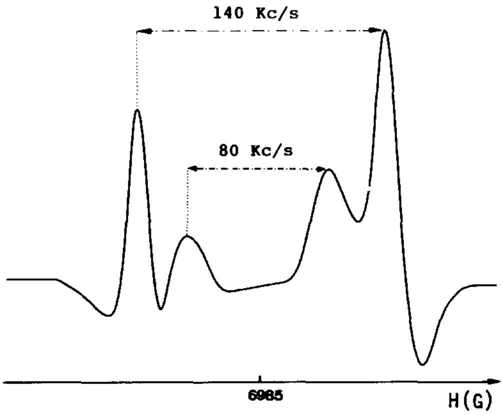

FIG. 7. Shape of the resonance line at 8 Mc/sec for $Na_2InZr(PO_4)_3$.

This being so, the quadrupolar coupling constant is obtained from the simple expression (*14*)

$$\nu^2 = \frac{144\nu_0\Delta\nu}{25I(I+1) - \frac{3}{4}}$$

where $\nu_Q = e^2qQ/2h$ for $I = \frac{3}{2}$, eQ is the quadrupolar momentum of ^{23}Na, eq the electric field gradient at the Na nucleus, $I = \frac{3}{2}$ the spin of ^{23}Na, ν_0 is the working frequency (here $\nu_0 = 8$ Mc/sec), and $\Delta\nu$ is the observed splitting of the central line due to second-order quadrupolar effect. Hence one obtains $\nu_Q = 1.47$ Mc/sec, value nearly independent on temperature and composition (Fig. 8). The very small decrease of ν_Q (<1%) with increasing x for a given temperature does not appear significant, nor the very small increase of ν_Q with T for a given concentration.

The analysis of the line corresponding to Na^+ in the $M2$ site is more ambiguous. As a matter of fact, the local environment of sodium clearly does not exhibit an axial symmetry so that the asymmetry parameter η is unknown ($0 \leq \eta \leq 1$) (Fig. 3). Recently it has been shown that the splitting strongly depends on the value of η (*14*). Thus the observed splitting (80 kc/sec) for the $M2$ site does not inevitably correspond to a smaller electric field gradient at the Na nucleus, but rather to a nonzero value of η. Nevertheless it appears that the quadrupolar splitting (i.e., the electric field gradient at the $M2$ site) is composition independent.

Let us return to $NaZr_2(PO_4)_3$ at high temperature: the extra line that appears above 400 K seems to be due to a migration of some sodium ions from $M1$ to another site, with an exchange slow enough to allow both sites to be well distinguished. Nevertheless the value of the splitting is much lower than that characterizing the sodium ions in $M2$ site in $Na_{1+x}In_xZr_{2-x}(PO_4)_3$.

A neutron diffraction study of γ-$Na_3Cr_2(PO_4)_3$ at 573 K recently performed by Soubeyroux has shown the existence of a small residual electronic density in the center of the ACGE polyhedron ($x = 0.98$, $y = 0.84$, $z = 0.96$) (Fig. 3) (*15*). This position will be called here $M5$. Moreover all crystallographic studies realized on Nasicon-type materials have shown a very high thermal agitation factor for Na^+ ($M1$) in the xOy plane. It can be thought that at 413 K a small amount of Na^+ occupies this new site. Kohler and Schulz have shown that in $Na_{3.10}Zr_{1.78}Si_{1.24}P_{1.76}O_{12}$ the limiting bottleneck between the $M1$ and $M2$ positions is the *ACG* triangle rather than *ACE* (*4*, *5*). A similar result has been found for γ-$Na_3Cr_2(PO_4)_3$.

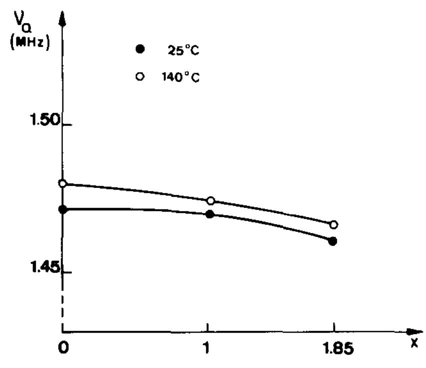

FIG. 8. Variation of quadrupolar effect constant vs composition and temperature.

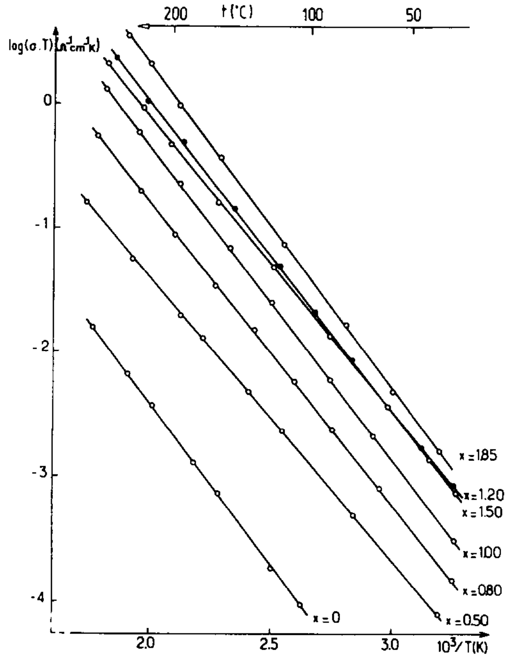

FIG. 9. Variation of the logarithm of the σT product vs reciprocal temperature.

All these facts emphasize the hypothesis of a relative occupancy of the site localized in the center of the *ACGE* polyhedron. A high-temperature neutron diffraction study of $NaZr_2(PO_4)_3$ is in progress to confirm this Na^+ distribution.

We have pointed out the quite anomalous behavior of $NaZr_2(PO_4)_3$ at 21 Mc/sec with respect to the classical models describing the influence of the atomic diffusion on the NMR linewidth. At present we cannot explain this behavior unless we assume that mechanisms other than diffusion are responsible for the relaxation (*11*).

Ionic Mobility of Na^+

At 8 Mc/sec the spectra are nearly temperature independent, but at 21 Mc/sec a line narrowing is observed above 250 K for $Na_{1+x}Zr_{2-x}In_x(PO_4)_3$ ($x > 0$) (Fig. 4). This behavior is due to Na^+ jumps whose frequency is higher than the intrinsic linewidth, i.e., $\nu_j \gtrsim 3 \times 10^4$ sec^{-1} at 250 K. The narrowing is unobservable at 8 Mc/sec probably because the spectra width is due to second-order quadrupolar effect ($\nu_Q \simeq$ 1.5 Mc/sec).

Starting from the value $\nu_j = 3 \times 10^4$ sec^{-1} one can calculate the related conductivity value using the Nernst-Einstein equation $\sigma/D = Nq^2/kT$ where the diffusion coefficient D is obtained from the NMR jump frequency ν_j according to the relation $D = l^2\nu_j/6$ (where N is the number of mobile ions per volume unit, q their charge, and l the jump distance).

This calculation has been made for the $Na_{2.5}In_{1.5}Zr_{0.5}(PO_4)_3$ composition ($N = 10^{22}$ Na^+ ions/cm^3) and $l = 3.3$ Å. At 250 K (line narrowing temperature) the calculated conductivity is 4 10^{-7} Ω^{-1} cm^{-1}, the value of which is not too far from the extrapolated experimental one: $\sigma_{\text{exp}} = 4\ 10^{-8}\ \Omega^{-1}\ \text{cm}^{-1}$ (Fig. 9).

Figure 10 shows the variation of the line-

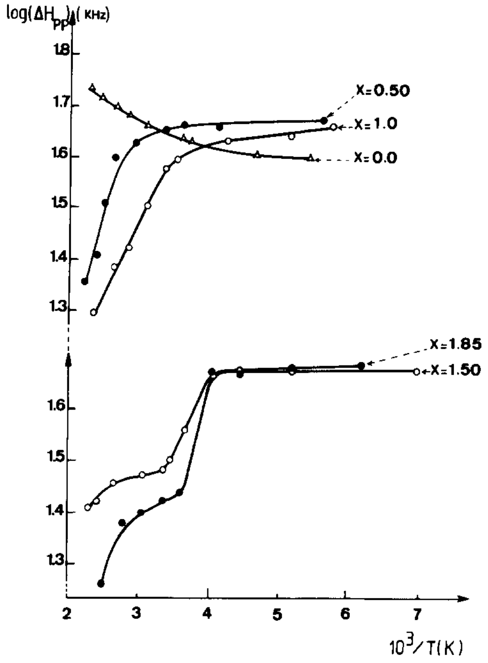

FIG. 10. Variation of the linewidth logarithm vs reciprocal temperature.

width logarithm vs reciprocal temperature for the various compositions investigated. Those corresponding to $x = 1.5$ and $x = 1.85$ clearly exhibit a narrowing occurring in two steps, as if two diffusion mechanisms coexist, the first one prevailing at low temperature, the second one at high temperature. The latter should appear at higher temperature for $x = 0.5$ and $x = 1$.

Two diffusion methods have been proposed: direct *M*2–*M*2 or indirect *M*1–*M*2–*M*1 transfers. Tran Qui *et al.* have shown that the first is predominant in the nonvacancy $Na_4Zr_2Si_4O_{12}$ compound, while the second appears at high temperature ($t >$ 620°C) (*3*). On the contrary for $Na_{3.10}Zr_{1.78}Si_{1.24}P_{1.76}O_{12}$, Kohler and Schulz have shown that the indirect transfer is already prevailing at 300°C.

The comparison of the sizes of the bottlenecks in γ-$Na_3Cr_2(PO_4)_3$ at 300°C indicates an easier diffusion by the indirect pathway. Furthermore the small occupancy of the *M*5 position is in accordance with this assumption as the *M*5 site is situated in the *M*1–*M*2 pathway.

In any case the two steps observed during the NMR line narrowing can be related to these two diffusion mechanisms.

General Discussion

From the previous results it is interesting to discuss the variation of the conductivity with the Na^+ rate in the skeleton. As shown in Fig. 9 the conductivity strongly increases when alkali ions are inserted in the framework: that of $Na_{2.85}Zr_{0.15}In_{1.85}(PO_4)_3$ is about 500 times higher than that of $NaZr_2(PO_4)_3$. Furthermore it should be noticed that the activation energy remains nearly constant.

From this conductivity difference on one hand and the strong Na^+ localization at *RT* in the *M*1 site for the $NaZr_2(PO_4)_3$ composition on the other hand, one can conclude that in this phase only a small amount of Na^+ participates in the conduction process.

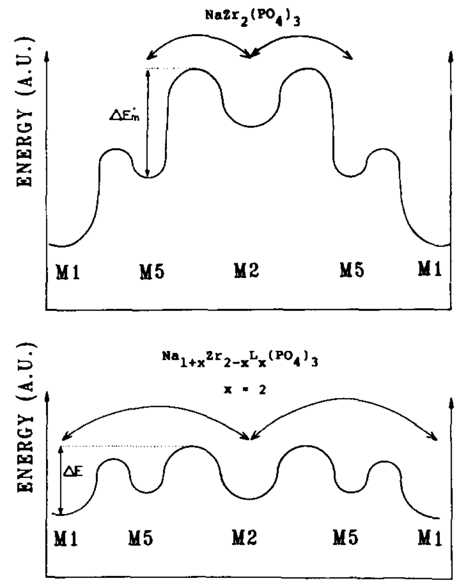

FIG. 11. Potential barrier modifications due to increasing sodium rates.

Whatever the Na^+ transfer considered, one can assume the occurrence of a high-energy interstitial site in $NaZr_2(PO_4)_3$ as the activation energy remains nearly constant ($\simeq$0.5 eV) for the overall solid solution. This result agrees with the existence of the new site detected by NMR at 410 K. Its occupancy increases with temperature. We have made the assumption that this site is the *M*5 one (center of the *ACGE* polyhedron) found in γ-$Na_3Cr_2(PO_4)_3$ at high temperature.

The activation energy determined for $NaZr_2(PO_4)_3$ $\Delta E'm$ corresponds to a migration energy, the energy difference between *M*1 and the interstitial *M*5 site being not involved. Figure 11 shows the energy scheme.

For sodium rates exceeding 1, Na^+–Na^+ interactions lead to a progressive delocalization of Na^+ ions in the two types of sites *M*1 and *M*2. The intensity of this interaction (i.e., the delocalization) is directly related to the sodium content. As a result the energy difference between the *M*1 and *M*2 sites decreases, the lowest value being obtained in the vicinity of three Na$^+$ ions by formula. In this case all alkali ions participate in the conduction process. This behavior is general and explains the conductivity evolution of all $Na_{1+x}(L, L')(PO_4)_3$ systems.

References

1. J. B. Goodenough, H. Y-P. Hong, and J. A. Kafalas, *Mat. Res. Bull.* **11,** 203 (1976).
2. H. Y-P. Hong, *Mat. Res. Bull.* **11,** 173 (1976).
3. D. Tran Qui, J. J. Capponi, M. Gondrand, M. Saib, J. G. Joubert, and R. D. Shannon, *Solid State Ionics* **3/4,** 219 (1981).
4. H. Kohler, H. Schulz, and O. Melnikov, *Mat. Res. Bull.* **18,** 589 (1983).
5. H. Kohler, H. Schulz, and O. Melnikov, *Mat. Res. Bull.* **18,** 1143 (1983).
6. F. d'Yvoire, M. Pintard-Screpel, E. Bretey, and M. de la Rochere, *Solid State Ionics 9/10,* 851 (1983).
7. M. Pintard-Srepel, F. d'Yvoire, and F. Remy, *C.R. Acad. Sci. C* **286,** 381 (1978).
8. C. Delmas, R. Olazcuaga, F. Cherkaoui, R. Brochu, and G. le Flem, *C.R. Acad. Sci. C* **287,** 169 (1978).
9. C. Delmas, J. C. Viala, R. Olazcuaga, G. Le Flem, F. Cherkaoui, R. Brochu, and P. Hagenmuller, *Solid State Ionics* **3/4,** 209 (1981).
10. C. E. Hayes and D. C. Ailion, Proceedings of the Conference "Fast Ion Transport in Solids" (P. Vashista, C. N. Mundy, and G. K. Shenoy, Eds.), p. 297, Lake Geneva, Wis., 1979.
11. D. T. Amm and S. L. Segel, *Solid State Ionics* **8,** 155 (1983).
12. L. O. Hagman and P. Kierkegaard, *Acta Chem. Scand.* **22,** 1822 (1968).
13. M. Guyot de la Rochere, Thesis, University of Paris VI (1984).
14. M. H. Cohen and F. Reiff, *Solid State Phys.* **5** (1957).
15. G. Lucazeau, M. Barj, J. L. Soubeyroux, A. J. Dianoux, and C. Delmas, *Solid State Ionics,* in press.